Printed soft skin electrodes for seamless bio-impedance measurements

1

Printed soft skin electrodes for seamless bio-impedance measurements

Bara Levit[1,2], Peter Krebsbach[3,4], Chen Bar-Haim[1], Gerardo Hernandez-Sosa[3,4,5], Yael Hanein[1,6,7,8,*]

1 School of Electrical Engineering, Tel Aviv University, Tel Aviv, Israel **2** School of Physics, Tel Aviv University, Tel Aviv, Israel **3** Light Technology Institute, Karlsruhe Institute of Technology (KIT), Karlsruhe, Germany **4** InnovationLab, Heidelberg, Germany **5** Institute of Microstructure Technology, Karlsruhe Institute of Technology (KIT), Eggenstein-Leopoldshafen, Germany **6** Tel Aviv University Center for Nanoscience and Nanotechnology, Tel Aviv University, Tel Aviv, Israel **7** Sagol School of Neuroscience, Tel Aviv University, Tel Aviv, Israel
8 X-trodes, Herzelia, Israel

* yaelha@tauex.tau.ac.il

Abstract

Bio-impedance measurements are widely used to assess various physiological parameters. Contemporary skin electrodes for bio-impedance measurements are cumbersome and novel electrode designs are needed to allow fast and easy placement, long-term stability and user comfort. This investigation introduces dry, printed, bio-compatible electrode arrays, made of screen-printed carbon and inkjet-printed PEDOT:PSS that measure bio-impedance non-invasively and stably. Two contact impedance measurements yield the lowest normalized values of soft electrodes reported to date. Four contact bio-impedance measurements from the radial, ulnar, common carotid and superficial temporal arteries were performed, demonstrating the ability to capture blood pulsation in different areas with small form factor. Owing to the unique properties of the printed electrodes reported here, we were able to demonstrate for the first time blood pulsation in the face, continuous blood pulsation measurement during simultaneous muscle activation and signal stability over many hours.

2

Introduction

Non-invasive bio-impedance measurements are used in a wide range of applications, including wound care [1], respiratory activity assessment [2] and monitering blood pressure [3]. Across these different applications, the need for wireless and wearable systems for long term and stable recordings is becoming widely recognized. Several lingering technological challenges limit the utilization of non-invasive bio-impedance measurements, including hardware miniaturization, data analysis and the large impedance of the skin-electrode interface. In particular, gel electrodes, which are commonly used in skin bio-impedance measurements to reduce the skin-electrode impedance, are notoriously challenging: they are bulky, dry out, tend to be unstable, and may cause skin irritation and discomfort to the user.

In recent years, much attention was directed to the implementation of alternative electrodes. In particular, several approaches based on dry conducting electrodes (e.g. silver, aluminum, copper, carbon) were investigated [4, 5, 6, 7, 8]. However, the aforementioned dry electrodes have limited flexibility and do not conform with the skin, resulting in relatively bulky and unstable systems. To improve conformity with the skin and stability, alternative materials and fabrication approaches were explored. For example, graphene-based temporary tattoo electrodes were fabricated using a thin-film process and exhibit high conformity to the skin [9, 10]. Other suggested electrode designs include screen and stencil printing on textiles [11] (used in wet form), electrode arrays printed on composite nanocellulose-polyurethane substrates [1], and inkjet-printed gold electrode arrays [12]. Owing to the limited performances of existing methods, impedance measurements were so far restricted to large and easily accessible regions, such as the forearm, legs and the neck and to short recording sessions [13]. Presently, there are no widely accepted low-impedance soft electrodes compatible with scalable manufacturing for ongoing impedance measurements.

With their excellent manufacturability properties, screen-printed carbon and inkjet-printed poly(3,4-ethylene dioxythiophene):polystyrene sulfonate PEDOT:PSS are ideal candidates for wearable bio-impedance applications. Both inks can be printed on soft films, such as polyurethane, to form highly conformal electrode arrays [14]. Printed carbon electrodes were studied extensively in recent years for a wide range of applications. In the realm of wearable devices, screen-printed carbon electrodes were studied for bio-chemical analysis of sweat [15] and for a wide range of electro-physiological applications [16] including: sleep assessment [17], high-resolution facial electromyography (EMG)[18, 19], facial EMG in lie detection [20] and electroencephalogram (EEG) [16]. Similarly, printed PE-DOT:PSS electrodes have been developed for applications such as multi-electrode arrays for in vitro cell studies [21], biochemical sensors [22] and electrodes for skin applications. In

3

the latter field, wearable devices made from printed PEDOT:PSS were studied for various bio-electronic applications, including ECG [23], EMG [24], facial EMG [14] and EEG monitoring [25, 26]. Although PEDOT:PSS films are attracting a lot of attention, their overall performances as skin electrodes are relatively modest, owing to delamination of thin films and instability under high-humidity due to swelling of the hygroscopic, but non-conductive PSS (supplementary **??** [27, 28, 29, 30]).

In this paper we explore screen-printed carbon and inkjet-printed (PEDOT:PSS) on polyurethane for the realization of state-of-the-art dry bio-impedance electrodes, specifically impedance plethysmography (IPG). IPG capitalizes on changes in conductivity during pulsation: Owing to mechanical changes in blood vessel geometry, blood pulsation is manifested as an impedance change [31]. We demonstrate process optimization, design considerations and bio-impedance measurements from the forearm, neck and face. Both approaches yield soft electrodes that conform with the skin with low contact impedance. We compare the contact impedance results to values measured for standard commercial gel electrodes, and demonstrate that the dry electrodes reach lower specific contact impedance values (normalized by area), compared with gel electrodes and previously reported dry electrodes. Four probe bio-impedance measurements were also performed to characterize the tissue bio-impedance at close proximity to the arteries. We demonstrate long-term (up to 13 hr) and stable monitoring of blood pulsation Finally, to demonstrate the robustness of the electrodes, we show how blood pulsation can be detected during muscle action close to the measurement site.

Materials and Methods

Commercial pre-gelled Ambu Commercial pre-gelled Ambu electrodes of 40 mm in diameter (Ambu® BlueSensor Q ECG electrodes) were used. These electrodes contain a wet gel area in the silver/silver chloride sensor region, including an adhesive surrounding area to stick them onto the skin, with easy access to a BNC connector for the bio-impedance measurements.

Screen-printed carbon electrodes Screen-printed carbon electrodes for electrophysiological and bio-impedance measurements were fabricated, as described previously [16, 19]. First, electrodes traces were screen-printed with silver ink (Creative Materials, 125-13T) on a 50 and 80 μm polyurethane sheet (Breathable transparent medical grade polyurethane / urethane / TPU film on paper carrier from DelStar Technologies, inc.; Figure 1(a)). Following silver printing, the films were dried on a heater at 50 °C for 15 min. Subsequently, carbon electrodes (124-50T and C200, Creative Materials) were printed in alignment with

4

the silver traces. Furthermore, the printed electrodes were dried again on the heating plate at 50 °C for 15 min. After printing, traces were passivated with a double adhesive 80 μm PU film (from Delstar EU94DS) which was cut to leave the carbon electrodes exposed. For impedance measurements, the arrays were bonded to metallic traces on a custom-made printed circuit board (PCB) which was designed to support BNC connections.

Inkjet-printed PEDOT:PSS electrodes A PixDro LP50 inkjet printer (Süss MicroTec SE) was used to fabricate silver - PEDOT:PSS dry electrodes on TPU substrates (figure 1(b)). The substrates were of the same type as the ones used for the screen-printed samples (80 μm). Before printing, the substrates were heated in a vacuum oven (120 °C for 10 min, 5 mbar, Memmert VO) and subsequently treated in an Ar plasma oven (Pico, Diener) for 30 s to optimize ink wetting. The silver ink (Silverjet, Sigma-Aldrich) was filtered through a 0.45 μm PVDF filter and deposited with a Sapphire QS-256/10 AAA printhead (drop volume of 10 pL, Fujifilm) set to a resolution of 1000 dpi. The deposited wet silver films were cured on a hotplate at 120 °C for 5 min resulting in a sheet resistance of $5 \pm 2 \, \Omega/\square$ and a layer thickness of 370 ± 130 nm. The latter was extracted from scanning electron microscopy (SEM, Zeiss Auriga System) images that can be found in the SI (figure **??**).

Before the PEDOT:PSS deposition, samples were treated with an additional 60 s of Ar plasma. Next, a commercially available PEDOT:PSS ink (Clevios F HC Solar, Heraeus) was filtered (0.45 μm PVDF), degassed in an ultra sonic bath for 20 min and printed with a Dimatix Materials Cartridge (10 pL, Fujifilm) that was set to a resolution of 1200 dpi. The samples were then placed on a hotplate at 120 °C for 10 min to obtain PEDOT:PSS layers of 100 ± 20 nm thickness (SEM images in figure **??**). The sheet resistance of PEDOT:PSS on bare TPU and on silver was measured to be around $150 \pm 10 \, \Omega/\square$ and $2.3 \pm 0.4 \, \Omega/\square$, respectively. The utilized PEDOT:PSS ink includes a low percentage of (3-Glycidoxy-propyl)methyldiethoxysilane in its formulation. Similar to published work on thermal crosslinking of PEDOT:PSS by addition of (3-Glycidyloxypropyl)trimethoxysilane, we achieved PEDOT:PSS films exhibiting a higher resistance to water and delamination than pristine PEDOT:PSS after the annealing process [32, 33]. For details of the crosslinking process, see the corresponding section in the SI. The final passivation steps, with double-sided adhesive and mounting on a PCB, were performed analogously to the screen-printed carbon electrodes.

Data collection

Two and four-terminal measurements were performed with an impedance analyzer (MFIA by Zurich Instruments) on the skin of 3 healthy volunteers (ages 27-28). IPG measurements were performed using a four-electrode array to exclude the significantly larger contact

5

impedance from the measurement (two inner sensing electrodes and two outer excitation electrodes, figure 1). The array was connected to a custom-made PCB with four BNC connections, which were connected to the impedance analyzer. AC current with a frequency between 10-100 kHz was applied between the outer electrodes, and the voltage was measured between the inner electrodes.

Data analysis

All IPG data was analyzed with python. The signals were processed using a second-order Butterworth band-pass filter with low and high frequency cut-offs at 0.5 and 6 Hz. The characteristic points of the pulse shape that were calculated were: the peak, through and maximum slope (MS). The average unnormalized CI was evaluated over the different layouts (i.e. different shapes, geometries and sizes).

Results

Carbon and PEDOT:PSS electrodes of different shapes (square and circle) and different inter-electrode spacing were printed using screen and inkjet-printing on thin PU films. The PEDOT:PSS films were tailored specifically to achieve stability (see Methods section) and adhesion, which is mandatory for stable recordings from the skin. In figure 1(d), we show two such arrays after placement on the forearm. As a reference, we also show an the commercial gel electrodes placed at the same region. Even though the printed electrodes are used in their dry form, their compact and flexible structure result in a conformal attachment to the skin, as evident in the stable two- and four-terminal measurements we describe below.

Contact impedance (CI) of four different electrode types (dry PEDOT:PSS, dry carbon, carbon with gel, and standard wet electrode (Ambu)) was measured and normalized by the electrode area (figure 2(a)). As CI depends on skin properties, an accurate comparison of CI of different electrodes mandates measurements at the same location. We used the location of the inner forearm (over the radial and ulnar arteries), as this area is most commonly used for wearable bio-impedance measurements. For completeness, we show contact impedance measurements at low frequencies (10-1000 Hz) in the supplementary ??.

Unnormalized, the commercial gel electrode has the lowest CI, followed by the gelled carbon. Carbon electrodes appear to have a lower CI compared to the PEDOT:PSS. By normalizing the CI data by area, we note the impact of size on the CI (figure 2(a2), (b2), and (c2)): While the wet electrode had lower CI compared to the dry electrodes before normalization, after normalizing, its specific impedance is in fact higher than the
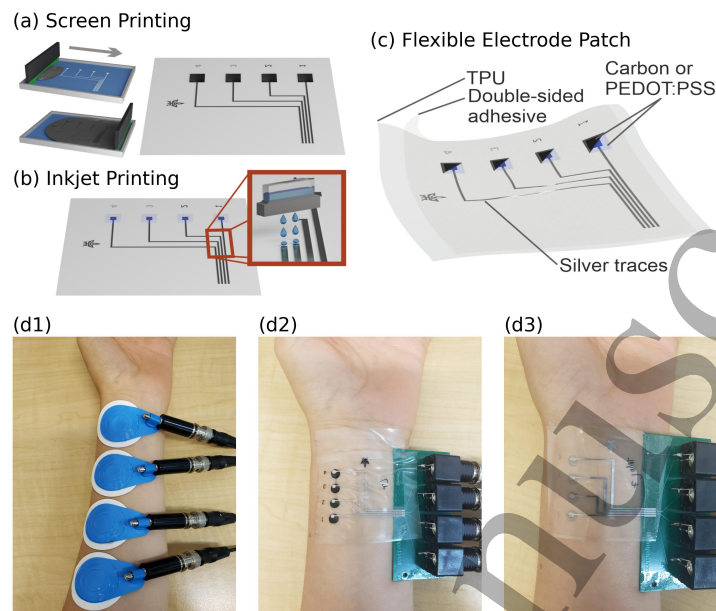
Figure 1: Printed skin electrodes for bio-impedance measurements. The two fabrication techniques applied in this study: (a) Screen printing of silver and carbon layers; and (b) inkjet-printed silver and PEDOT:PSS layers. (c) A schematic of a complete array with passivation. (d1) Commercial gel electrodes placed on the arm. (d2) Dry printed carbon electrode array placed on the arm. (d3) Dry printed PEDOT:PSS electrode array placed on the arm.

dry electrodes for frequencies above 10 kHz. At 10 kHz, the unnormalized CI of carbon, PEDOT:PSS and the gel electrodes is $\sim$6.4, $\sim$13 and $0.51\,\text{k}\Omega$ respectively (values for carbon and PEDOT:PSS electrodes were averaged over a range of geometries, shapes, and sizes). The areas included in the CI measurements ranged from $\sim$13 to $\sim$28 mm^2. To the best of our knowledge the dry carbon electrodes described here have the lowest CI values reported to date for soft electrodes (with the largest electrode ($\sim$28 mm^2), reaching CI of $3.1\,\text{k}\Omega$ at $10\,\text{kHz}$).

To evaluate the stabilization of the CI, we measured it every 15 min after placement on the skin (figure 2(b-c)). We observed a large jump in CI between '0 min' (right when placing the array) and '15 min' (15 min after placing the array). After 15 min, the changes were less significant. We hypothesize that the large jump represents the time it takes the material to properly adhere onto the skin surface (improving charge transfer between the electrode and the skin interfaces).

We now turn to four-terminal impedance measurements to demonstrate IPG. In IPG,
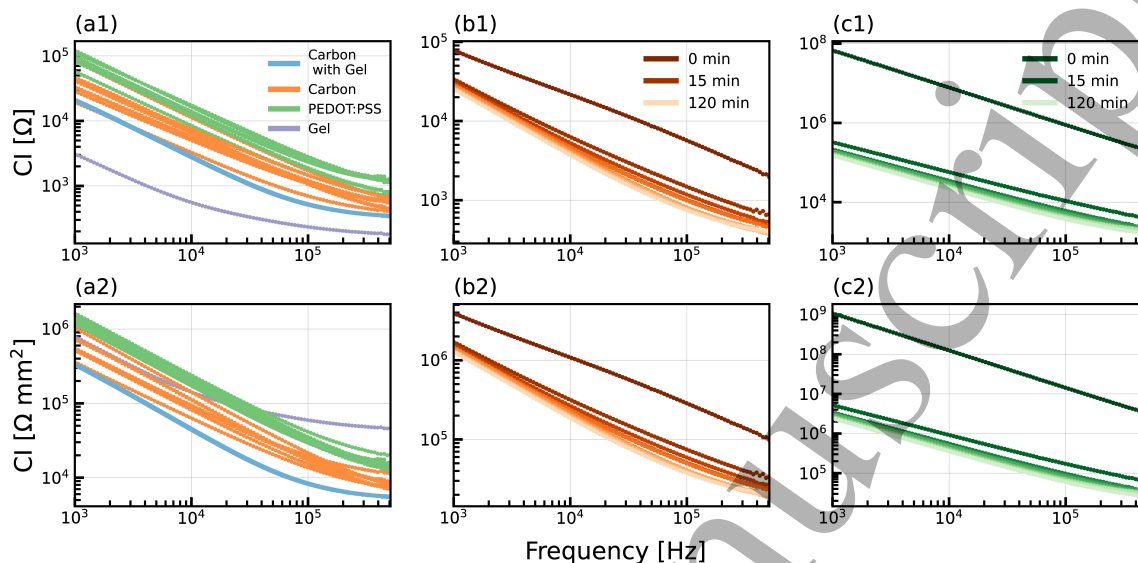
Figure 2: **Contact Impedance Comparison.** (a1) Contact impedance over the radial artery for carbon (with and without gel), PEDOT:PSS and gel electrodes. Each dotted line is a measurement taken with a different array (in terms of geometry, size and shape), as well as different days. (b1) Contact impedance time dependence for carbon electrodes (c1) Contact impedance time dependence for PEDOT:PSS electrodes. (a2-c2) Normalized contact impedance of (a1-c1) by area of the electrode.

the measured impedance reflects artery volume [31]: As blood pulsates through arteries, the artery volume changes. Since blood is conductive, the artery can be modeled as a cylindrical resistor. When the artery expands (as a result of the pulse), it effectively becomes equivalent to a cylindrical resistor with a larger radius. In terms of impedance, this translates to decrease in the impedance of the artery, and the impedance of the overall measured segment.

Figure 3 shows four-terminal IPG measurements with commercial wet electrodes, wet and dry carbon electrodes and dry PEDOT electrodes. Baseline impedance was in the range of 61 and 140-140 Ω to 170 Ω for the commercial and printed electrodes, respectively, reflecting the difference in their geometries. The change in the IPG signal was 0.03 and 0.13 Ω for the commercial and the printed electrodes, respectively. The smaller dimensions of the printed electrodes contributed to stronger sensitivity. Peaks, troughs and maximum slope points for each pulse were successfully detected and marked automatically. These characteristics are commonly used to evaluate the impedance change, which translates to

8
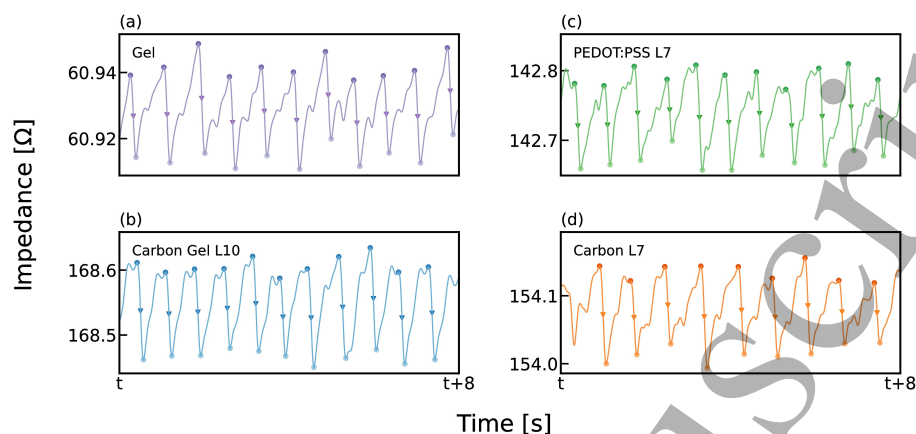
Figure 3: **Blood pulsation measured with commercial wet electrodes and printed electrodes.** Four-terminal impedance versus time under static conditions (f = 74.2 kHz). Electrodes were placed close to the radial artery. (a)-(b) Gel electrodes signals: (a) Commercial gel electrodes (b) Gelled carbon electrodes (layout 10). (c)-(d) Dry electrodes signals: (c) PEDOT:PSS (layout 7), (d) Carbon (layout 7)

the volume change of the artery, as well as the pulse transit time (PTT) which can be used to evaluate blood pressure [34]. Both electrode types measure the same phenomena, albeit the printed electrodes achieve the measurement with dramatically smaller form factor. In particular, the printed electrodes in their dry form offer excellent performances along with long term stability (up to 13 hr supplementary figure **??**).

Owing to their soft and dry nature, the electrodes can be conveniently placed at almost any hair-free area of the skin. In particular, the locations of the radial and ulnar arteries (at the forearm), the common carotid artery (at the neck) and the superficial temporal artery (at the face), are of particular interest in many physiological investigations. In figure 4 we show carbon and PEDOT:PSS electrode arrays placed at these locations and their corresponding blood pulsation measurements. In all locations we observe clear pulsation signals. At the forearm, a prominent secondary notch (the dicrotic notch [35], signifying the back reflection of the pressure pulse due to higher vascular resistance) is observed [36]. As expected, at the neck and face this feature appears to be less pronounced and the shape of the pulse is different. It is evident that pulse shape has a strong association with the electrode location [2].

Blood pulsation was also measured during muscle activation to demonstrate electrode stability under dynamic conditions. In figure 5, we show four-terminal measurements of gel

9
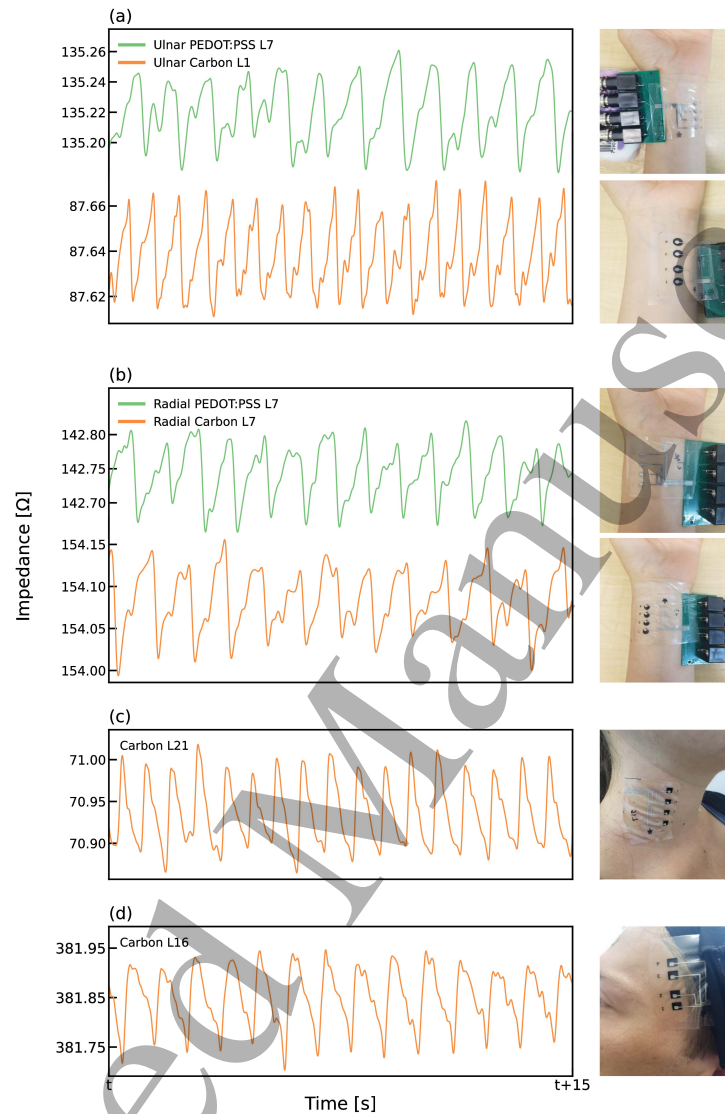
Figure 4: Four-terminal impedance vs. time measured from the hand, neck and face (f = 74.2 kHz). Electrode positions are shown on the right. (a) Radial artery measurement with PEDOT:PSS (top) and carbon (bottom) electrodes. (b) Ulnar artery measurement with PEDOT:PSS (top) and carbon (bottom) electrode. (c) Common carotid artery measurement with carbon electrodes. (d) Superficial temporal artery measurement with carbon electrodes.

(top) and dry carbon (bottom) electrodes during relaxed conditions (left) and fist clenching

10
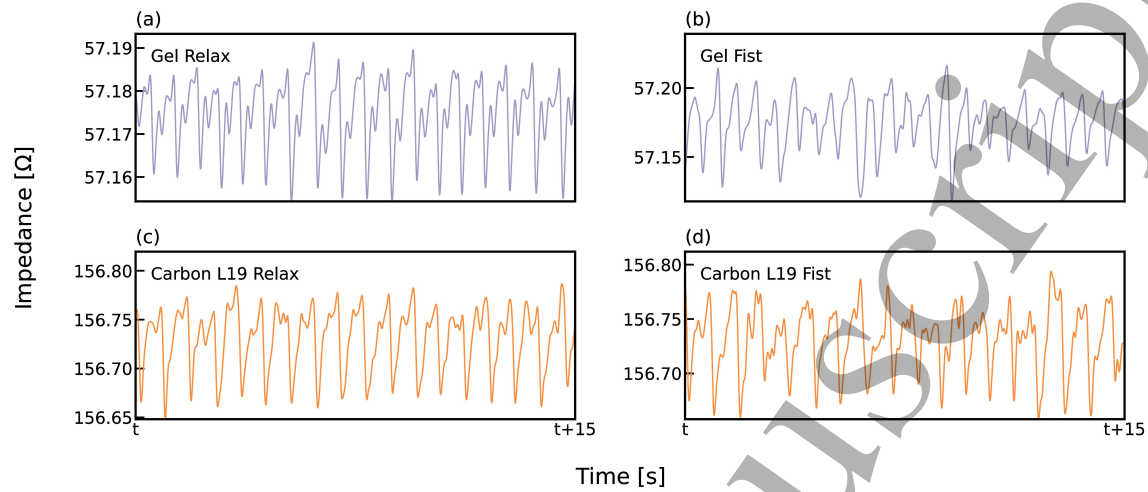
Figure 5: Wet and dry electrodes under dynamic conditions (f = 74.2 kHz). **Electrodes were placed close to the ulnar artery and data were recorded during** **relaxation and fist clenching. (a) Commercial gel electrodes signal during** **relaxation. (b) Commercial gel electrodes signal during fist clenching. (c) Dry** **printed carbon electrodes signal during relaxation. (d) Dry printed carbon** **electrodes signal during fist clenching.**

(right). The electrodes were placed over the same forearm that was clenching the fist, over the ulnar artery. A clear pulse is detectable during fist clenching for both electrodes.

Finally an important parameter that impacts bio-impedance measurements is the electrode design (e.g. shape, dimensions and distance) [5] [37]. In this investigation, printed electrodes were realized and measured in a range of geometries, shapes and sizes. Although we could identify differences in pulse amplitude and shape the variability between measurements were greater than between sessions proving that physiological variability has greater contribution than variability between electrode arrays. This large variability is a major challenge in assessing the effect of array design on performances and a more methodical investigation is needed, possibly by averaging measurements over many sessions and subjects.

Discussion

Our investigation reports on dry printed electrode arrays for bio-impedance measurements. We demonstrated low contact impedance values and stable four-terminal impedance measurements. We successfully detected pulsation at rest and during muscle activation and

11

long term stability. The results we presented here show state-of-the-art performances and a path towards wearable bio-impedance devices as an alternative to the cumbersome gel electrode.

To assess the performances of the arrays, we measured pulsation from four different arteries: the radial, the ulnar, the common carotid and the superficial temporal arteries. In addition, to test the versatility and stability of the electrodes, we performed IPG measurements during muscle actions. The actions included: Fist clenching when measuring from the radial and ulnar arteries and facial expressions while measuring the superficial temporal artery (data not shown).

In this investigation we studied two alternative printing approaches with similar performances. Inkjet-printing of PEDOT:PSS is widely used and is a convenient approach for rapid prototyping and personalized electrode arrays that can be tailored for each subject, depending on particular physiological features. Film adhesion of printed inkjet PEDOT:PSS is challenging and special care was used in this investigation regarding the stability of the array. Further improvement can be made to the electrical connection of the silver traces to read-out electronics. Given the layer thickness of 100 nm, traces are prone to break when stretched or bent against hard surfaces (such as rigid PCBs), increasing their electrical resistance. Screen-printed carbon is easier to implement, and scale-up is straight forward. However, its suitability for rapid prototyping is more challenging.

The results presented here can benefit a wide range of applications. In particular, the measurement of blood flow and pressure is of special significance [38]. Monitoring changes in blood flow is of critical importance in many fields: From medicine [39] [40], to psychology [41] [42], [43] [44] and cosmetic surgery [45]. Invasive and non-invasive monitoring of blood flow is widespread in clinical diagnostics. As abnormal blood flow may be episodic in nature and may not be manifested in clinical settings, wearable solutions for on-going monitoring at home is a major need. Two commonly used techniques for wearable and non-invasive blood flow detection are photoplethysmography (PPG) and IPG. Both are sensitive to blood volume changes. Whilst IPG capitalizes on changes in conductivity during pulsation, PPG monitors the increase in blood in the artery segment during pulsation [46] utilizing changes in light absorption of the tissue. At each pulsation, the increase in blood results in a measurable change in the transmitted or reflected light. Both techniques can be used not just to record the pulsation, but also to extract blood pressure, and thus have attracted huge interest. Although offering similar insight, IPG and PPG differ fundamentally: Deep penetration to the tissue is possible with IPG, due to the high-frequency current, but PPG is limited to the skin surface. Deep penetration allows higher accuracy in detection of the blood volume change, as well as providing detailed characteristics of the

12

haemodynamic parameters [35][9][10].

The main overreaching gap our technology helps address is the realization of fully independent skin devices, suited for ongoing bio-impedance monitoring under realistic conditions, while still maintaining process compatibility with industrial fabrication methods. A fully wearable bio-impedance system requires additional components such as: Low power micro-electronics, improved data analysis approaches [10] and proper coupling between the soft electronics and the wireless data acquisition system. The soft and dry electrodes we presented demonstrate an important step towards this goal.

Wearable devices are becoming an important building block as a digital health solution. They allow on-going monitoring of various parameters, ranging from electrophysiology, heart rate, blood pressure, to name just a few examples. Wearable sensors benefit both patients and the medical system compared with traditional practices. In particular, information can be collected quickly and continuously under realistic conditions and visits to the clinic can be minimized. In the new reality imposed by the Covid-19 crisis, home-based patient monitoring is becoming critically important. The lighter and seamless the technology is, the higher are the chances that it will be widely used and accepted. Simultaneously, it must provide medically validated information that will be trusted by the medical community and by medical practitioners.

REFERENCES   13

References

[1] Colm Mc Caffrey, Jacek Flak, Kaisa Kiri, and Pekka Pursula. Flexible bioimpedance spectroscopy system for wound care monitoring. *BioCAS 2019 - Biomedical Circuits and Systems Conference, Proceedings*, pages 1–4, 2019. doi:10.1109/BIOCAS.2019.8919095.

[2] Kaan Sel, Deen Osman, and Roozbeh Jafari. Non-Invasive Cardiac and Respiratory Activity Assessment from Various Human Body Locations Using Bioimpedance. *IEEE Open Journal of Engineering in Medicine and Biology*, 2:210–217, 2021. ISSN 26441276. doi:10.1109/OJEMB.2021.3085482.

[3] Sudipta Ghosh, Bhabani Prasad Chattopadhyay, Ram Mohan Roy, Jayanta Mukherjee, and Manjunatha Mahadevappa. Non-invasive cuffless blood pressure and heart rate monitoring using impedance cardiography. *Intelligent Medicine*, 2(4):199–208, 2022. ISSN 2667-1026. doi:https://doi.org/10.1016/j.imed.2021.11.001. URL https://www.sciencedirect.com/science/article/pii/S2667102621001194.

[4] Deen Osman, Matija Jankovic, Kaan Sel, Roderic I. Pettigrew, and Roozbeh Jafari. Blood pressure estimation using a single channel bio-impedance ring sensor. In *2022 44th Annual International Conference of the IEEE Engineering in Medicine I& Biology Society (EMBC)*, pages 4286–4290, 2022. doi:10.1109/EMBC48229.2022.9871653.

[5] Jesse F. Phipps, Kaan Sel, and Roozbeh Jafari. Arterial pulse localization with varying electrode sizes and spacings in wrist-worn bioimpedance sensing. In *2022 44th Annual International Conference of the IEEE Engineering in Medicine I& Biology Society (EMBC)*, pages 2886–2890, 2022. doi:10.1109/EMBC48229.2022.9871270.

[6] Min-Chang Cho, Jee-Yeon Kim, and Seong Hwan Cho. A bio-impedance measurement system for portable monitoring of heart rate and pulse wave velocity using small body area. In *2009 IEEE International Symposium on Circuits and Systems (ISCAS)*, pages 3106–3109, 2009. doi:10.1109/ISCAS.2009.5118460.

[7] Toan Huu Huynh and Wan-Young Chung. Radial electrical impedance: A potential indicator for noninvasive cuffless blood pressure measurement. *Journal of Sensor Science and Technology*, 26(4):239–244, 2017. doi:https://doi.org/10.5369/JSST.2017.26.4.239.

[8] Hip Kõiv, Ksenija Pesti, Mart Min, Raul Land, and Indrek Must. Comparison of the carbon nanofiber-/fiber- and silicone-based electrodes for bioimpedance measurements. *IEEE Transactions on Instrumentation and Measurement*, 69(4):1455–1463, 2020. doi:10.1109/TIM.2019.2962297.

[9] Kaan Sel, Dmitry Kireev, Alexander Brown, Bassem Ibrahim, Deji Akinwande, and Roozbeh Jafari. Electrical characterization of graphene-based e-tattoos for bio-

REFERENCES

14

impedance-based physiological sensing. In *2019 IEEE Biomedical Circuits and Systems Conference (BioCAS)*, pages 1–4, 2019. doi:10.1109/BIOCAS.2019.8919003.

[10] Dmitry Kireev, Kaan Sel, Bassem Ibrahim, Neelotpala Kumar, Ali Akbari, Roozbeh Jafari, and Deji Akinwande. Continuous cuffless monitoring of arterial blood pressure via graphene bioimpedance tattoos. *Nature nanotechnology*, 17(8):864–870, 2022. ISSN 1748-3387.

[11] Manoj Jose, Marijn Lemmens, Seppe Bormans, Ronald Thoelen, and Wim Deferme. Fully printed, stretchable and wearable bioimpedance sensor on textiles for tomography. *Flexible and Printed Electronics*, 6(1), 2021. ISSN 20588585. doi:10.1088/2058-8585/abe51b.

[12] Yasser Khan, Felippe J. Pavinatto, Monica C. Lin, Amy Liao, Sarah L. Swisher, Kaylee Mann, Vivek Subramanian, Michel M. Maharbiz, and Ana C. Arias. Inkjet-printed flexible gold electrode arrays for bioelectronic interfaces. *Advanced Functional Materials*, 26(7):1004–1013, 2016. doi:https://doi.org/10.1002/adfm.201503316. URL https://onlinelibrary.wiley.com/doi/abs/10.1002/adfm.201503316.

[13] Ahmad Hammoud, Alexey Tikhomirov, Galina Myasishcheva, Zein Shaheen, Alexander Volkov, Andrey Briko, and Sergey Shchukin. Multi-channel bioimpedance system for detecting vascular tone in human limbs: An approach. *Sensors*, 22(1), 2022. ISSN 1424-8220. doi:10.3390/s22010138. URL https://www.mdpi.com/1424-8220/22/1/138.

[14] Lilah Inzelberg, M.D. Moshe David Pur, Stefan Schlisske, Tobias Rödlmeier, Omer Granoviter, David Rand, Stanislav Steinberg, Gerardo Hernandez-Sosa, and Yael Hanein. Printed facial skin electrodes as sensors of emotional affect. *Flexible and Printed Electronics*, 3(4), 2018. ISSN 20588585. doi:10.1088/2058-8585/aae252.

[15] Kerstin Malzahn, Joshua Ray Windmiller, Gabriela Valdés-Ramírez, Michael J. Schöning, and Joseph Wang. Wearable electrochemical sensors for in situ analysis in marine environments. *Analyst*, 136(14):2912–2917, 2011. ISSN 13645528. doi:10.1039/c1an15193b.

[16] L. Inzelberg and Y. Hanein. Electrophysiology meets printed electronics: The beginning of a beautiful friendship. *Frontiers in Neuroscience*, 12, 2019. ISSN 1662453X. doi:10.3389/fnins.2018.00992.

[17] Shiran Shustak, Lilah Inzelberg, Stanislav Steinberg, David Rand, Moshe David Pur, Inbar Hillel, Shlomit Katzav, Firas Fahoum, Maarten De Vos, Anat Mirelman, and Yael Hanein. Home monitoring of sleep with a temporary-tattoo EEG, EOG and EMG electrode array: A feasibility study. *Journal of Neural Engineering*, 2019. ISSN 17412552. doi:10.1088/1741-2552/aafa05.

[18] Lilah Inzelberg, David Rand, Stanislav Steinberg, Moshe David-Pur, and Yael Hanein. A wearable high-resolution facial electromyography for long term recordings in freely

REFERENCES   15

behaving humans. *Sci Rep*, 8(1):2058, Feb 2018. ISSN 2045-2322 (Electronic); 2045-2322 (Linking). doi:10.1038/s41598-018-20567-y.

[19] Lilah Inzelberg, Moshe David-Pur, Eyal Gur, and Yael Hanein. Multi-channel electromyography-based mapping of spontaneous smiles. *J Neural Eng*, 17(2):026025, Apr 2020. ISSN 1741-2552 (Electronic); 1741-2552 (Linking). doi:10.1088/1741-2552/ab7c18.

[20] Anastasia Shuster, Lilah Inzelberg, Ori Ossmy, Liz Izakson, Yael Hanein, and Dino J. Levy. Lie to my face: An electromyography approach to the study of deceptive behavior. *Brain and Behavior*, (August):1–12, 2021. ISSN 21623279. doi:10.1002/brb3.2386.

[21] Leonardo D Garma, Laura M Ferrari, Paola Scognamiglio, Francesco Greco, and Francesca Santoro. Inkjet-printed pedot: Pss multi-electrode arrays for low-cost in vitro electrophysiology. *Lab on a Chip*, 19(22):3776–3786, 2019.

[22] Chakrit Sriprachuabwong, Chanpen Karuwan, Anurat Wisitsorrat, Ditsayut Phokharatkul, Tanom Lomas, Pornpimol Sritongkham, and Adisorn Tuantranont. Inkjet-printed graphene-pedot: Pss modified screen printed carbon electrode for biochemical sensing. *Journal of Materials Chemistry*, 22(12):5478–5485, 2012.

[23] Eloïse Bihar, Timothée Roberts, Mohamed Saadaoui, Thierry Hervé, Jozina B De Graaf, and George G Malliaras. Inkjet-printed pedot: Pss electrodes on paper for electrocardiography. *Advanced healthcare materials*, 6(6):1601167, 2017.

[24] Eloise Bihar, Timothee Roberts, Yi Zhang, Esma Ismailova, Thierry Herve, George G Malliaras, Jozina B De Graaf, Sahika Inal, and Mohamed Saadaoui. Fully printed all-polymer tattoo/textile electronics for electromyography. *Flexible and Printed Electronics*, 3(3):034004, 2018.

[25] Aikaterini Marinou, Rachel Saunders, and Alexander J Casson. Flexible inkjet printed sensors for behind-the-ear ssvep eeg monitoring. In *2020 IEEE International Conference on Flexible and Printable Sensors and Systems (FLEPS)*, pages 1–4. IEEE, 2020.

[26] Laura M Ferrari, Usein Ismailov, Jean-Michel Badier, Francesco Greco, and Esma Ismailova. Conducting polymer tattoo electrodes in clinical electro-and magneto-encephalography. *npj Flexible Electronics*, 4(1):1–9, 2020.

[27] Lorenz Bießmann, Lucas Philipp Kreuzer, Tobias Widmann, Nuri Hohn, Jean-François Moulin, and Peter Müller-Buschbaum. Monitoring the swelling behavior of pedot: Pss electrodes under high humidity conditions. *ACS applied materials & interfaces*, 10(11):9865–9872, 2018.

[28] Mahmut Kuş and Salih Okur. Electrical characterization of pedot: Pss beyond humidity saturation. *Sensors and Actuators B: Chemical*, 143(1):177–181, 2009.

REFERENCES   16

[29] Xinyan Tracy Cui and David Daomin Zhou. Poly (3, 4-ethylenedioxythiophene) for chronic neural stimulation. *IEEE Transactions on Neural Systems and Rehabilitation Engineering*, 15(4):502–508, 2007.

[30] Chung-Ki Cho, Woo-Jin Hwang, Kyoungtae Eun, Sung-Hoon Choa, Seok-In Na, and Han-Ki Kim. Mechanical flexibility of transparent pedot: Pss electrodes prepared by gravure printing for flexible organic solar cells. *Solar Energy Materials and Solar Cells*, 95(12):3269–3275, 2011.

[31] Jan Nyboer. *Electrical impedance plethysmography : the electrical resistive measure of the blood pulse volume, peripheral and central blood flow.* C.C. Thomas, Springfield, Ill., 2nd ed.. edition, 1970.

[32] Mohammed Elmahmoudy, Sahika Inal, Anne Charrier, Ilke Uguz, George G Malliaras, and Sébastien Sanaur. Tailoring the electrochemical and mechanical properties of pedot: Pss films for bioelectronics. *Macromolecular Materials and Engineering*, 302 (5):1600497, 2017.

[33] Anna Håkansson, Shaobo Han, Suhao Wang, Jun Lu, Slawomir Braun, Mats Fahlman, Magnus Berggren, Xavier Crispin, and Simone Fabiano. Effect of (3-glycidyloxypropyl) trimethoxysilane (gops) on the electrical properties of pedot: Pss films. *Journal of Polymer Science Part B: Polymer Physics*, 55(10):814–820, 2017.

[34] Roman Kusche, Arthur-Vincent Lindenberg, Sebastian Hauschild, and Martin Ryschka. Aortic frequency response determination via bioimpedance plethysmography. *IEEE Transactions on Biomedical Engineering*, 66(11):3238–3246, 2019. doi:10.1109/TBME.2019.2902721.

[35] Synthetic photoplethysmography of the radial artery through parallelized monte carlo and its correlation to body mass index, 2020. ISSN 1537-1409.

[36] Bassem Ibrahim and Roozbeh Jafari. Cuffless blood pressure monitoring from an array of wrist bio-impedance sensors using subject-specific regression models: Proof of concept. *IEEE Transactions on Biomedical Circuits and Systems*, 13(6):1723–1735, 2019. doi:10.1109/TBCAS.2019.2946661.

[37] Ting-Wei Wang, Wen-Xiang Chen, Hsiao-Wei Chu, and Shien-Fong Lin. Single-channel bioimpedance measurement for wearable continuous blood pressure monitoring. *IEEE Transactions on Instrumentation and Measurement*, 70:1–9, 2021. doi:10.1109/TIM.2020.3035578.

[38] Sudipta Ghosh, Bhabani Prasad Chattopadhyay, Ram Mohan Roy, Jayanta Mukherjee, and Manjunatha Mahadevappa. Non-invasive cuffless blood pressure and heart rate monitoring using impedance cardiography. *Intelligent Medicine*, 2021. ISSN 2667-1026. doi:https://doi.org/10.1016/j.imed.2021.11.001. URL https://www.sciencedirect.com/science/article/pii/S2667102621001194.

REFERENCES   17

[39] Salim S Virani, Alvaro Alonso, Emelia J Benjamin, Marcio S Bittencourt, Clifton W Callaway, April P Carson, Alanna M Chamberlain, Alexander R Chang, Susan Cheng, Francesca N Delling, et al. Heart disease and stroke statistics—2020 update: a report from the american heart association. *Circulation*, 141(9):e139–e596, 2020. doi:https://doi.org/10.1161/CIR.0000000000000757.

[40] DJ Ewing, IW Campbell, and BF Clarke. Mortality in diabetic autonomic neuropathy. *The Lancet*, 307(7960):601–603, 1976. doi:https://doi.org/10.1016/S0140-6736(76)90413-X.

[41] Ruth E. Propper, Sean E. McGraw, Tad T. Brunyé, and Michael Weiss. Getting a grip on memory: Unilateral hand clenching alters episodic recall. *PLOS ONE*, 8(4): 1–4, 04 2013. doi:10.1371/journal.pone.0062474. URL https://doi.org/10.1371/journal.pone.0062474.

[42] T. Iida, M. Kato, O. Komiyama, H. Suzuki, T. Asano, T. Kuroki, T. Kaneda, P. Svensson, and M. Kawara. Comparison of cerebral activity during teeth clenching and fist clenching: a functional magnetic resonance imaging study. *European Journal of Oral Sciences*, 118(6):635–641, 2010. doi:https://doi.org/10.1111/j.1600-0722.2010.00784.x. URL https://onlinelibrary.wiley.com/doi/abs/10.1111/j.1600-0722.2010.00784.x.

[43] Daniel N. McIntosh R. B. Zajonc Peter S. Vig Stephen W. Emerick. Facial movement, breathing, temperature, and affect: Implications of the vascular theory of emotional efference. *Cognition and Emotion*, 11(2):171–196, 1997. doi:10.1080/026999397379980. URL https://doi.org/10.1080/026999397379980.

[44] Daniel N. McIntosh. Facial feedback hypotheses: Evidence, implications, and directions. *Motivation and emotion*, 20(2):121–147, 1996. ISSN 0146-7239.

[45] Sebastian Cotofana, Natalia Lowry, Aditya Devineni, Gianna Rosamilia, Thilo L. Schenck, Konstantin Frank, Sana A. Bautista, Jeremy B. Green, Hassan Hamade, and Robert H. Gotkin. Can smiling influence the blood flow in the facial vein?— an experimental study. *Journal of Cosmetic Dermatology*, 19(2):321–327, 2020. doi:https://doi.org/10.1111/jocd.13247. URL https://onlinelibrary.wiley.com/doi/abs/10.1111/jocd.13247.

[46] Cheng Wang, Zhangjun Li, and Xunbin Wei. Monitoring heart and respiratory rates at radial artery based on ppg. *Optik*, 124(19):3954–3956, 2013. ISSN 0030-4026. doi:https://doi.org/10.1016/j.ijleo.2012.11.044. URL https://www.sciencedirect.com/science/article/pii/S0030402613000120.